Preservation of near-solar neon isotopic ratios in Icelandic basalts

Eleanor T. Dixon [a],*, Masahiko Honda [a], Ian McDougall [a],
Ian H. Campbell [a], Ingvar Sigurdsson [b]

[a] *Research School of Earth Sciences, The Australian National University, Canberra, ACT 0200 Australia*
[b] *Nature Conservation Agency, Hlemmur 3, P.O. Box 5324, 125 Reykjavik, Iceland*

Abstract

Neon isotopic ratios measured in olivine and basaltic glass from Iceland are the most primitive observed so far in terrestrial mantle-derived samples. Ratios were measured in gas released from olivine and basaltic glass from a total of 10 samples from the Reykjanes Peninsula, Iceland, and one sample from central Iceland. The neon isotopic ratios include solar-like, mid-ocean ridge basalt (MORB)-like and atmospheric compositions. Neon isotopic ratios near the air–solar mixing line were obtained from the total gas released from glass separates from five samples. MORB-like neon isotopic compositions were measured in the total gas released from olivine and glass separates from four samples. Although there is clear evidence for a solar neon component in some of the Icelandic samples, there is no corresponding evidence for a solar helium ratio ($320R_a > {}^3He/{}^4He > 100R_a$). Instead, ${}^3He/{}^4He$ ratios are mainly between $12 \pm 2(R_a)$ and $29 \pm 3(R_a)$, similar to the range observed in ocean island basalts, indicating that the He–Ne isotopic systematics are decoupled. The mantle source of Icelandic basalts is interpreted to be highly heterogeneous on a local scale to explain the range in observed helium and neon isotopic ratios. The identification of solar-like neon isotopic ratios in some Icelandic samples implies that solar neon trapped within the Earth has remained virtually unchanged over the past ~ 4.5 Ga. Such preservation requires a source with a high [Ne_{solar}]/[U+Th] ratio so that the concentration of solar neon overwhelms the nucleogenic ${}^{21}Ne^*$ produced from the decay of U and Th in the mantle over time. High [Ne_{solar}]/[U+Th] ratios are unlikely to be preserved in the mantle if it has experienced substantial melting. An essentially undegassed primitive mantle component is postulated to be the host of the solar neon in the Icelandic plume source. Relatively small amounts of this primitive mantle component are likely to mix with more depleted and degassed mantle such that the primitive mantle composition is not evident in other isotopic systems (e.g. strontium and neodymium). The lower mantle plume source is inferred to be relatively heterogeneous owing to being more viscous and less well stirred than the upper mantle. This discovery of near-solar neon isotopic ratios suggests that relatively primitive mantle may be preserved in the Icelandic plume source. © 2000 Elsevier Science B.V. All rights reserved.

Keywords: Iceland; noble gases; cosmogenic elements; helium; neon

1. Introduction

Analyses of helium and neon isotopes in samples from ocean island basalts (OIBs) and mid-

* Corresponding author. Tel.: +61-2-6249-3959;
Fax: +61-2-6249-3683; E-mail: eleanor.dixon@anu.edu.au

ocean ridge basalts (MORBs) have provided evidence that the Earth's mantle preserves components of primordial gases (e.g. [1,2]). The primordial helium and neon in terrestrial samples are believed to be solar in composition and to have been augmented over the course of the Earth's history by the coupled production of radiogenic ^4He and nucleogenic ^{21}Ne ($^{21}Ne*$) from the decay of U and Th in the mantle [3]. Radiogenic ^4He is produced by α decay from U and Th and some of these α particles collide with oxygen to produce $^{21}Ne*$. The ^3He, ^{20}Ne and ^{22}Ne in the mantle are dominantly primordial, so that the mantle helium and neon isotopic ratios are controlled by the ratios of [primordial ^3He]/[U+Th] and [primordial Ne]/[U+Th], respectively.

Previous investigations of helium and neon isotopic compositions of samples from OIBs and MORBs suggest that the OIB sources have higher relative [primordial ^3He]/[U+Th] and [primordial Ne]/[U+Th] ratios than those of MORBs for two reasons. First, the maximum measured $^3He/^4He$ ratios in OIBs, such as in Hawaii ($32R_a$, where R_a is the atmospheric $^3He/^4He$ ratio) (e.g. [4]) and Iceland ($37R_a$) [5] are higher than generally found in MORBs (average value, $8.5 \pm 1.4(R_a)$) (e.g. [6]). Second, the mixing trends between mantle and atmospheric ('air') neon compositions defined by OIBs are closer to the slope of the air–solar mixing line in the neon three-isotope plot ($^{20}Ne/^{22}Ne$ versus $^{21}Ne/^{22}Ne$) than those of MORBs (e.g. [7] and references therein). In other words, the more solar-like neon isotopic ratios in OIBs suggest a higher solar to nucleogenic neon ratio (e.g. $^{22}Ne_{solar}/^{21}Ne*$) than in MORBs. OIBs show a large range in helium and neon isotopic compositions. In contrast, the helium and mantle-endmember neon isotopic ratios are relatively uniform in MORBs, suggesting that the MORB source reservoir is comparatively well mixed [8].

This study investigates the noble gas isotopic compositions of some Icelandic basalts. Previous studies of Icelandic basalts revealed $^3He/^4He$ ratios greater than $30R_a$ [5] that exceed the maximum ratios measured in Hawaiian basalts. The characteristically primitive neon isotopic ratios found in Hawaiian basalts are expected owing to the coupling of helium and neon isotope system-

atics in the mantle [3]. For this reason, relatively primitive neon isotopic ratios are also expected in Icelandic basalts. Thus, one of the primary aims of this study was to determine whether Icelandic basalts have primitive neon isotopic ratios.

We present helium and neon isotopic ratios on gases extracted from olivine and glass separates from youthful and relatively primitive Icelandic picrites and tholeiitic basalts. Surprisingly, the neon isotopic ratios from some Icelandic samples lie within the experimental error of the air–solar mixing line, implying that they are more solar-like than ratios found in Hawaiian basalts. This implies that parts of the Icelandic plume source have a higher [Ne_{solar}]/[U+Th] ratio than the Hawaiian plume source. The means by which solar-like neon isotopic ratios may be preserved over the Earth's history are discussed. The argon, krypton and xenon results obtained in the course of this investigation will be presented elsewhere.

1.1. Geologic setting

Iceland lies along a segment of the Mid-Atlantic Ridge (MAR) associated with high basaltic magma production (Fig. 1). The volcanic activity is much more voluminous than that which is generally associated with MAR spreading [9] and causes Iceland to have a greater elevation and greater maximum crustal thickness (ca. 25 km) than normal oceanic crust (7 km) [10]. The high eruption rate and distinctive geochemistry of Icelandic volcanism [11], including the higher $^3He/^4He$ ratios relative to adjacent MORBs [12], are consistent with a mantle plume origin for the enhanced Icelandic volcanism. Additional evidence from seismic tomography studies support a plume origin for Iceland (e.g. [13] and references therein) and suggest that it may originate from as deep as the core–mantle boundary [14,15].

The neovolcanic zones on Iceland (NVZ) (Fig. 1) are tectonically active zones of recent volcanism and rifting, which extend through the Reykjanes Peninsula (the western NVZ) and central Iceland and continue through northern Iceland (the northern NVZ). There are two off-axis rift zones, the Snaefellsnes and the eastern volcanic zones (SVZ and EVZ), where erupted basalts
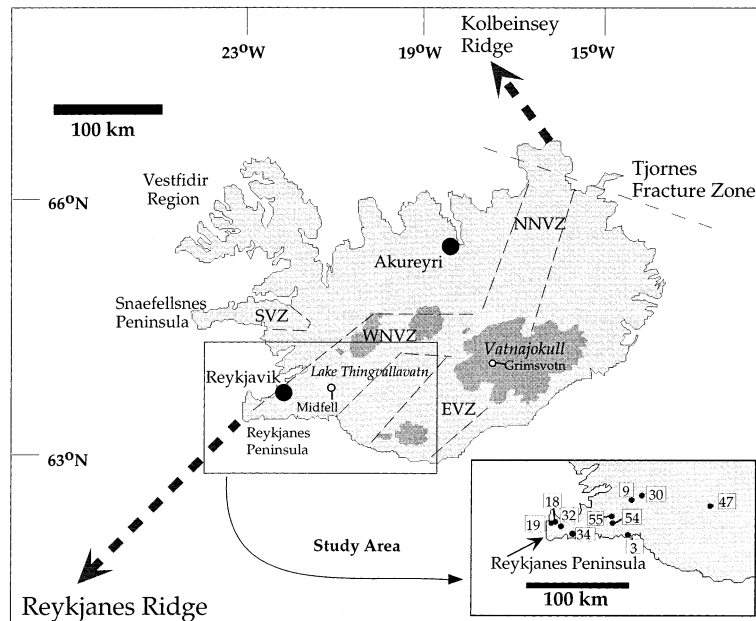
Fig. 1. Map of Iceland. The Reykjanes and Kolbeinsey Ridges to the south and north of Iceland extend onto land to become the NVZ, shown as regions bounded by the lightly dashed lines. The portion of the NVZ that passes through the Reykjanes Peninsula is the western NVZ (WNVZ), which joins the off-axis eastern VZ (EVZ) near Vatnajökull to become the northern NVZ (NNVZ). The NNVZ is offset by the Tjornes fracture zone and then continues offshore to become the Kolbeinsey Ridge. The off-axis Snaefellsnes VZ (SVZ) and glaciers (jökulls) (darker gray areas) are also shown. Inset: the area of study, SW Iceland, including the Reykjanes Peninsula and part of the EVZ. Sample localities are indicated, without the 'ice-' prefix of the sample number.

are chemically distinct from those in the NVZs [16]. Because the MAR/NVZ is an active spreading centre, the oldest rocks in Iceland ($\sim$16 Ma) (e.g. [17]) are at the greatest distance from the NVZ. Those closer to the NVZ are generally younger basalts (e.g. [18]). Picritic and tholeiitic lavas along the Reykjanes Peninsula close to and within the NVZ are very young and predominantly postglacial (ca. 12 ka) [16]. Basalts erupted beneath glaciers commonly form pillow basalts with quenched, glassy rims that are good targets for noble gas studies.

1.2. Previous noble gas investigations in Iceland and adjacent MAR

The ^{3}He/^{4}He ratios of basaltic samples from along the MAR to the north (Kolbeinsey Ridge) and south (Reykjanes Ridge) of Iceland increase with proximity to Iceland [12]. In the south, they increase from values ($9.3R_a$) that are close to typical MORB ratios ($8.5R_a$) at 53°N to a maximum of $16R_a$ just south of the Reykjanes Peninsula, and suggest that close to Iceland, a higher proportion of plume-derived helium, with high ^{3}He/^{4}He ratios, has mixed with MORB-derived helium [12].

Helium studies of Icelandic samples from the Reykjanes Peninsula (western NVZ), the NW Peninsula of Iceland, the EVZ and northern NVZ, [5,19–21] have shown a range in ^{3}He/^{4}He ratios ($4 < R_a < 37$). Most basaltic and geothermal samples from the Reykjanes Peninsula have ^{3}He/^{4}He ratios that are similar to the maximum value ($16R_a$) from MORB samples obtained along the Reykjanes Ridge closest to Iceland [19,22]. A relatively high ^{3}He/^{4}He ratio of $30R_c/R_a$ (R_c = air corrected) has been measured in hydrothermal water in Iceland's northwest peninsula (Vestfidir) [23] (Fig. 1). The most active volcanism in Iceland occurs beneath Vatnajokull (Fig. 1) at Grimsvötn, where ^{3}He/^{4}He ratios are $\sim$19R_c/R_a [22]. Evi-

dently, comparing the $^3He/^4He$ ratios in hydrothermal water from the Vestfidir region with those from Grimsvötn, the maximum measured $^3He/^4He$ ratios are not necessarily focused at the location of greatest volcanic activity. In comparison, the lowest $^3He/^4He$ ratios measured in Iceland ($3R_a$), from geothermal samples and intermediate and silicic volcanic glasses, have been interpreted to result from the release of radiogenic ^4He from the uppermost basaltic crust into the water or magma [20,23]. Whether crustal contamination is the main factor responsible for the heterogeneous $^3He/^4He$ ratios has been debated; such variations in the $^3He/^4He$ ratios may alternatively be regarded as reflecting heterogeneities in the mantle beneath Iceland [21].

In contrast to the numerous helium studies, there is only one neon isotopic investigation of Icelandic basalts prior to the present study [24]. The neon isotopic ratios from an investigation of two samples from a single locality at Dagmalafell quarry, Midfell, in the Hengill volcanic system [24], define a trend in the neon three-isotope plot that is intermediate between the Loihi–Kilauea (L–K) line (e.g. [25]) and the MORB trend ([7] and references therein), with the highest ratio of $^{21}Ne/^{22}Ne = 0.047 \pm 0.005$ at a near-solar $^{20}Ne/^{22}Ne$ ratio of 13.7 ± 0.3 (solar $^{20}Ne/^{22}Ne$ ratio is 13.8 ± 0.1 [26]). The measured $^3He/^4He$ ratios are $15–19(R_a)$. Clearly, additional analyses of neon are required to further characterise the possible range in the neon isotopic ratios in Icelandic basalts.

2. Samples

2.1. Sample localities and sampling strategy

The picrites and olivine tholeiites used for noble gas analyses in this study were collected from eight localities along the Reykjanes Peninsula and from one locality in the EVZ (Fig. 1, inset). Picrites and olivine tholeiites were targeted because they contain olivines that can trap noble gases either in their glass inclusions or within their crystal lattices. In addition, picrites are mafic, high temperature lavas and are among the least

evolved rock types known in Iceland (e.g. [27]). Thus, these rocks are the best candidates for preserving mantle-derived noble gases. Quenched glasses from pillow basalts were also analysed as they contain relatively high concentrations of noble gases. The Reykjanes Peninsula lavas, from the western NVZ, were erupted in small dykes and shield volcanoes that are grouped into volcanic systems, or swarms. From southwest to northeast along the Reykjanes Peninsula, these are the Reykjanes, Grindavik, Krisuvik, Blafjoll and Hengill volcanic swarms [16]. Samples were collected from the Reykjanes (*ice-18*, *-19*), Grindavik (*ice-32.1*, *-32.2* and *-34*) and Hengill swarms (*ice-3*, *-9*, *-30*, *-54* and *-55*) (Table 1). Sample *ice-9* (olivine and glass) and the samples analysed by Harrison et al. ([24] and Harrison, personal communication) are from a quarry at the southern end of the Midfell volcanoes in the Hengill swarm [27,28]. Sample *ice-47* is from the EVZ in central Iceland.

Samples were collected from quarries, under large boulders in outcrops or from actively eroding cliff-faces, wherever possible, to reduce potential interferences from cosmogenically produced isotopes. Production of ^3He and ^{21}Ne by cosmic ray particle-induced spallation of nuclei in the rock matrix [29] decreases exponentially with depth below the exposed rock surface as a function of the absorption mean free path (175 to 155 g/cm) [30] and the rock density [31]. Hence, production of cosmogenic nuclides is substantially attenuated at depths of ~ 1 m below the surface. Details of the sample localities and depth below the surface from which the samples were taken are shown in Table 1. In localities where basaltic glasses were not well-shielded, the glasses were crushed under vacuum to release gases from the vesicles rather than the glass matrix, which might include cosmogenic isotopes. Noble gas results obtained during this study from samples that were only partly shielded from cosmic rays are not reported here as these samples may contain cosmogenic isotopes of helium and neon.

2.2. Sample descriptions and general petrography

The phenocryst phases in the picrite and olivine

Table 1
Sample descriptions

ANU#	Sample No.	Replicates	Locality	Latitude/ longitude	Analysis type	Material	Weight (g)	Rock type	Size fraction (mm)	Percent. vesicles	Comment	Depth (m)	Elevation (m)
96-745	ice-3	a	Burfell i olfusi	21°29'/ 63°55'	step-heat	olivine	3.384	picrite	$0.420 < x < 1$			quarry	150
96-745	ice-3	b			step-heat	olivine	2.786		$0.420 < x < 1$				
97-657	ice-9	a	Midfell	21°4'/ 64°11'	step-heat	olivine	5.162	picrite	$0.420 < x < 1$		minor px	quarry	300
97-657	ice-9	b			step-heat	olivine	5.160		$0.420 < x < 1$				
97-657	ice-9	c			step-heat	olivine	5.176		$0.420 < x < 1$				
97-657	ice-9	d			vac. cr.	olivine	0.702		$0.420 < x < 1$				
97-657	ice-9	g1			step-heat	glass	2.026		$1 < x < 2.36$	vesicle shards			
97-657	ice-9	g2			vac. cr.	glass	0.585		$0.420 < x < 1$	5–10%			
97-657	ice-9	g3			vac. cr.	glass	0.720		$0.420 < x < 1$	<5%	diff. split than -9g1.2		
97-666	ice-18	b	Stapafell	22°32'/ 63°55'	step-heat	olivine	3.649	ol. thol.	$0.420 < x < 1$				
97-666	ice-18	g2			step-heat	glass	3.704		$0.420 < x < 1$	<30%			
97-666	ice-18	g3			vac. cr.	glass	0.983		$1 < x < 2.36$	~30%			
97-667	ice-19	a	Sulur	22°32'/ 63°54'	step-heat	olivine	5.341	ol. thol.	$0.420 < x < 1$		pillow margin	active quarry	50
97-667	ice-19	b	Sulur		step-heat	olivine	5.153		$0.420 < x < 1$				
97-678	ice-30	a	Landamn-nahellir	20°54'/ 64°13'	step-heat	olivine	5.071	ol. thol.	$0.420 < x < 1$		pillow margin	> 2	100
97-680	ice-32.1	a	near Svart-sengisfell	22°26'/ 63°53'	step-heat	olivine	5.054	ol. thol.	$0.420 < x < 1$	<5%	dyke margin	> 2	sea-level
97-680	ice-32.2	g1			vac. cr.	glass	3.056	ol. thol.	$1 < x < 2.36$	<5%	pillow margin		sea-level
97-680	ice-32.2	g2			vac. cr.	glass	1.040		$1 < x < 2.36$	<5%	hyaloclastite		
97-682	ice-34	a	SW Skala-Maelifell	22°19'/ 63°15'	step-heat	olivine	3.556	ol-cpx thol.	$0.420 < x < 1$		abd. px	4	100
97-696	ice-47	g	Sigalda	19°10'/ 64°10'	vac. cr.	glass	0.921	thol.	$1 < x < 2.36$	~1%	pillow margin	> 2	500
97-703	ice-54	g	Lambafell	21°28'/ 64°1'	vac. cr.	glass	0.843	ol. thol.	$0.420 < x < 1$	<5%	pillow margin	quarry	300
97-704	ice-55	g	Kongsgil	21°25'/ 64°2'	vac. cr.	glass	0.818	ol. thol.	$0.090 < x < 1$	<5%	pillow margin	graded ski slope	300

The samples names are designated according to the following code: all olivine samples with replicates are given a label containing the sample number, e.g. ice-3, followed by an alphabetic character for each replicate, e.g. ice-3a, ice-3b, etc. Glasses are labelled with the suffix 'g', followed by a numeric character for each replicate, e.g. ice-18g2, ice-18g3. Different samples from the same locality are labelled with an extra digit in the sample number, e.g. ice-32.1g and -32.2g are from the same quarry, but are different samples. The type of sample (olivine/glass) and analysis (step-heating/crushing), sample localities, the grain size fraction used for the analysis and the visually estimated percent vesicles in glass samples are shown. The depth of the sample from the surface and outcrop elevation are noted to demonstrate the degree of shielding of the samples from cosmic rays.

Table 2
Helium and neon abundances and isotopic ratios

Sample	T (°C)	^{4}He cm^3 STP/g (1×10^{-10})	^{3}He/^{4}He (1×10^{-5})	R/R_a	^{22}Ne cm^3 STP/g (1×10^{-12})	^{20}Ne/^{22}Ne	^{21}Ne/^{22}Ne
ice-3a, 3.384 g, Burfell i Olfusi, olivine	900	b.c.	b.c.	b.c.	0.32 ± 0.04	11.21 ± 0.24	0.029 ± 0.003
	1800	b.c.	b.c.	b.c.	2.5 ± 0.1	10.30 ± 0.10	0.0295 ± 0.0005
	1850	b.c.	b.c.	b.c.	0.8 ± 0.1	9.77 ± 0.20	0.030 ± 0.003
	total	b.c.	b.c.	b.c.	3.6 ± 0.2	10.27 ± 0.08	0.0295 ± 0.0008
ice-3b, 2.786 g, Burfell i Olfusi, olivine	900	b.c.	b.c.	b.c.	0.67 ± 0.05	10.76 ± 0.18	0.029 ± 0.001
	1800	b.c.	b.c.	b.c.	0.42 ± 0.05	11.11 ± 0.27	0.032 ± 0.002
	1850	b.c.	b.c.	b.c.	b.c.	b.c.	b.c.
	total	b.c.	b.c.	b.c.	1.07 ± 0.07	10.97 ± 0.16	0.029 ± 0.001
ice-9a, 5.162 g, Burfell i Olfusi, olivine	900	13.3 ± 0.8	3.9 ± 0.8	28 ± 5	n.a.	n.a.	n.a.
	1800	72 ± 4	2.5 ± 0.3	18 ± 2	2.0 ± 0.1	11.96 ± 0.36	0.0308 ± 0.0007
	total	85 ± 4	2.7 ± 0.3	20 ± 2	2.0 ± 0.1	11.96 ± 0.36	0.0308 ± 0.0007
ice-9b, 5.160 g, Burfell i Olfusi, olivine	900	10.6 ± 0.6	4.1 ± 0.5	29 ± 3	0.34 ± 0.07	13.3 ± 1.1	0.034 ± 0.003
	1800	82 ± 5	4.1 ± 0.5	29 ± 3	b.b.	b.b.	b.b.
	1850	b.c.	b.c.	b.c.	0.49 ± 0.07	11.10 ± 0.46	0.031 ± 0.002
	total	93 ± 5	4.1 ± 0.4	29 ± 3	0.8 ± 0.1	11.98 ± 0.56	0.032 ± 0.002
ice-9c, 5.176 g, Burfell i Olfusi, olivine	900	13.1 ± 0.8	2.6 ± 0.2	19 ± 1	b.c.	b.c.	b.c.
	1800	66 ± 4	2.4 ± 0.2	17 ± 1	b.c.	b.c.	b.c.
	total	79 ± 4	2.4 ± 0.1	17 ± 1	b.c.	b.c.	b.c.
ice-9d, 0.702 g, Burfell i Olfusi, olivine	crush	117 ± 7	2.8 ± 0.2	20 ± 1	b.c.	b.c.	b.c.
ice-9g1, 2.026 g, Burfell i Olfusi, glass	700	1206 ± 70	2.3 ± 0.2	16 ± 1	11.1 ± 0.5	10.07 ± 0.14	0.0300 ± 0.0005
	1600	8122 ± 471	2.5 ± 0.2	18 ± 1	23 ± 1	10.81 ± 0.14	0.0301 ± 0.0006
	total	9327 ± 476	2.4 ± 0.2	17 ± 1	34 ± 1	10.57 ± 0.10	0.0301 ± 0.0004
ice-9g2, 0.585 g, Burfell i Olfusi, glass	crush	62375 ± 3619	2.7 ± 0.2	19 ± 1	181 ± 9	10.74 ± 0.13	0.0304 ± 0.0005
ice-9g3, 0.720 g, Burfell i Olfusi, glass	crush	23772 ± 1379	2.6 ± 0.2	19 ± 2	339 ± 15	9.94 ± 0.08	0.0295 ± 0.0003
ice-18b, 3.649 g, Stapafell, olivine	900	14.1 ± 0.8	2.4 ± 0.3	17 ± 2	17.9 ± 0.8	9.94 ± 0.08	0.0298 ± 0.0003
	1800	83 ± 5	2.3 ± 0.3	16 ± 2	0.64 ± 0.04	9.64 ± 0.25	0.029 ± 0.001
	total	97 ± 5	2.3 ± 0.2	16 ± 2	18.5 ± 0.8	9.93 ± 0.08	0.0298 ± 0.0003
ice-18g2, 3.704 g, Stapafell, glass	700	408 ± 24	1.8 ± 0.2	13 ± 2	55 ± 2	9.75 ± 0.08	0.0317 ± 0.0003
	1500	112 ± 7	2.5 ± 0.3	18 ± 2	36 ± 2	9.86 ± 0.08	0.0296 ± 0.0003
	total	520 ± 25	1.9 ± 0.2	14 ± 1	90 ± 3	9.79 ± 0.06	0.0309 ± 0.0002
ice-18g3, 0.983 g, Stapafell, glass	crush	619 ± 36	2.0 ± 0.2	14 ± 2	74 ± 3	10.01 ± 0.09	0.0299 ± 0.0003
ice-19a, 5.341 g, Sulur, olivine	900	20 ± 1	1.9 ± 0.2	14 ± 2	12.7 ± 0.6	9.87 ± 0.08	0.0299 ± 0.0003
	1800	90 ± 5	2.5 ± 0.3	18 ± 2	0.58 ± 0.05	10.79 ± 0.25	0.029 ± 0.002
	total	110 ± 5	2.4 ± 0.2	17 ± 2	13.3 ± 0.6	9.91 ± 0.08	0.0298 ± 0.0003
ice-19b, 5.1531 g, Sulur, olivine	900	14.5 ± 0.8	2.2 ± 0.2	16 ± 1	1.29 ± 0.06	9.82 ± 0.09	0.0291 ± 0.0003
	1800	131 ± 8	2.0 ± 0.2	15 ± 1	0.53 ± 0.04	10.46 ± 0.17	0.030 ± 0.001
	total	145 ± 8	2.1 ± 0.2	15 ± 1	1.81 ± 0.07	10.01 ± 0.08	0.0294 ± 0.0004
ice-30, 5.071 g, near Landamnahellir, olivine	900	8.4 ± 0.5	2.3 ± 0.2	17 ± 1	3.2 ± 0.2	10.19 ± 0.14	0.0300 ± 0.0005
	1800	68 ± 4	1.9 ± 0.1	14 ± 1	0.31 ± 0.03	11.72 ± 0.43	0.0299 ± 0.0016
	1850	7.7 ± 0.4	2.3 ± 0.2	17 ± 1	0.29 ± 0.03	11.85 ± 0.52	0.0345 ± 0.0019
	total	85 ± 4	2.0 ± 0.1	14.2 ± 0.8	3.8 ± 0.2	10.44 ± 0.13	0.0303 ± 0.0005
ice-32.1a, 5.054 g, near Svartengisfell, olivine	900	13.7 ± 0.8	1.6 ± 0.3	11 ± 2	15.4 ± 0.7	9.95 ± 0.08	0.0295 ± 0.0003
	1800	173 ± 10	2.1 ± 0.3	15 ± 2	3.5 ± 0.2	10.28 ± 0.10	0.0302 ± 0.0005
	total	187 ± 10	2.1 ± 0.2	15 ± 2	18.9 ± 0.7	10.01 ± 0.07	0.0296 ± 0.0003
ice32.2g1, 3.056 g, near Svartengisfell, glass	700	300 ± 17	1.7 ± 0.2	12 ± 1	65 ± 3	9.92 ± 0.08	0.0296 ± 0.0003
	1500	91 ± 5	2.0 ± 0.3	15 ± 2	14.1 ± 0.6	9.97 ± 0.09	0.0301 ± 0.0003
	total	391 ± 18	1.8 ± 0.2	13 ± 1	79 ± 3	9.93 ± 0.07	0.0297 ± 0.0003
ice-32.2g2, 1.040 g, near Svartengisfell, glass	crush	173 ± 10	2.5 ± 0.3	18 ± 2	35 ± 2	9.82 ± 0.08	0.0297 ± 0.0003
ice-34a, 3.556 g, Issolfsskah, SW of Skala Maelifell, olivine	900	3.3 ± 0.2	b.c.	b.c.	3.0 ± 0.2	10.16 ± 0.12	0.0300 ± 0.0005
	1800	35 ± 2	1.9 ± 0.2	14 ± 2	0.31 ± 0.06	10.52 ± 0.51	0.026 ± 0.002
	total	39 ± 2	1.7 ± 0.2	12 ± 2	3.3 ± 0.2	10.20 ± 0.12	0.0296 ± 0.0005

Table 2 (*continued*)

Sample	T (°C)	^{4}He cm^3 STP/g (1×10^{-10})	^{3}He/^{4}He (1×10^{-5})	R/R_a	^{22}Ne cm^3 STP/g (1×10^{-12})	^{20}Ne/^{22}Ne	^{21}Ne/^{22}Ne
ice-47g, 0.921 g, Sigalda, glass	crush	2928 ± 170	2.7 ± 0.3	20 ± 2	72 ± 3	9.84 ± 0.08	0.0300 ± 0.0003
ice-54g, 0.8426 g, Lambafell, glass	crush	214 ± 12	2.6 ± 0.2	19 ± 2	30 ± 1	9.92 ± 0.09	0.0311 ± 0.0006
ice-55g, 0.8184 g, Kongsgil, glass	crush	270 ± 26	2.8 ± 0.4	20 ± 3	20 ± 1	10.01 ± 0.09	0.0319 ± 0.0006

Abbreviations: 'b.b.' is below blank, 'b.c.' is below cut-off level (see Appendix A for explanation), and 'n.a.' is not analysed.

tholeiite measured in this study are olivine, spinel $\pm$ plagioclase $\pm$ clinopyroxene. The petrography and mineralogy of Reykjanes Peninsula samples (including those from the Midfell volcanoes in the Hengill system) have been presented in a number of studies (e.g. [16,27,28,32]). The sample collected at Midfell (*ice-9*) is from a locality where gabbroic nodules are incorporated in picritic basalts. The gabbroic nodules are composed of plagioclase, Al–Cr diopside and olivine [27,28]. The olivines used in this study are euhedral to subhedral, 2–8 mm in length, with abundant spinel inclusions and typically very few fluid inclusions, and variable amounts of melt inclusions [33]. The groundmass in most samples is comprised of plagioclase microlites in a finer grained matrix.

3. Analytical results

Details of the methods used to obtain the noble gas results are found in Appendix A. The helium and neon abundances and isotopic ratios from 11 different samples are reported here, including a total of 12 olivine and 10 glass separates (some samples have more than one replicate). (Note also that *ice-32.1* and *-32.2* are different samples.) Gases were released from most olivine separates by step-heating, whereas they were released from glasses by step-heating and/or crushing. Several grams of olivine were step-heated for each sample because of the low gas concentrations in olivine (Table 2). An explanation of the sample-labelling system can be found in the footnote of Table 1.

3.1. Helium

The ^{4}He abundances in Icelandic samples range

from 4×10^{-10} to 2×10^{-8} cm^3 STP/g in olivine and from 2×10^{-8} to 6×10^{-6} cm^3 STP/g in glass (Table 2 and Fig. 2). The olivine and glass samples have helium isotopic ratios that lie between $13 \pm 2(R_a)$ and $29 \pm 3(R_a)$ from step-heating or crushing analyses (Table 2). The majority of analyses of olivine and glass from step-heated and crushed samples yielded ^{3}He/^{4}He ratios between $12R_a$ and $20R_a$ (Table 2 and Fig. 2). Total gas isotopic ratios, obtained by combining the gas released during incremental step-heating, have a similar range to those from individual step-heating/crushing extractions (Table 1).

Most of the ^{3}He/^{4}He ratios from this study are similar to those found in previous studies on samples from nearby localities. For example, samples from Sigalda (*ice-47*, ^{3}He/^{4}He $= 20 \pm 2(R_a)$) and Stapafell (*ice-18g*, $14 \pm 2(R_a)$) have ^{3}He/^{4}He ratios
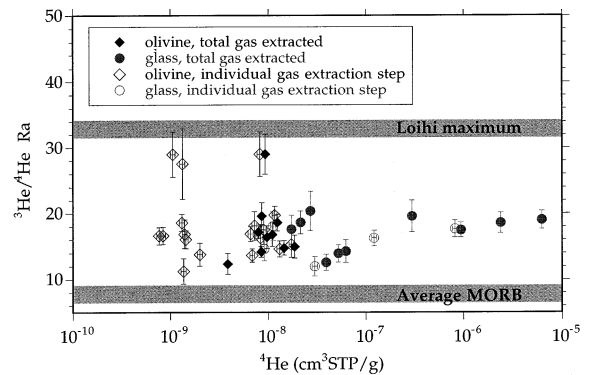
Fig. 2. Helium step-heating and crushing results for olivine and glass samples. The MORB ratio ($\sim 8.5R_a$) (e.g. [36]), and the maximum Loihi ratio ($33R_a$) [2,3] are also shown. The Icelandic results of ^{3}He/^{4}HeR_a versus ^{4}He concentration (cm^3 STP/g) shows that for a wide range in ^{4}He concentrations, most Icelandic samples lie between 12 and $20R_a$, and only the olivine separates *ice-9a*, *-b* have ^{3}He/^{4}He ratios of near $30R_a$. Uncertainty is 1σ.

similar to those from the same localities reported by Kurz et al. [21] ($20.8R_a$) and Condomines et al. [20] ($13.8 \pm 0.1(R_a)$), respectively. In contrast, the glass and olivine from a sample from Midfell (*ice-9*) have maximum $^3He/^4He$ ratios that are distinct from those measured in a different Midfell sample (*MIDgl, -ol, -cr1, -cr2*) by Burnard et al. [19]. The olivine sample from this study has $^3He/^4He$ ratios of near $29 \pm 3(R_a)$ in *ice-9a, -b*, but lower ratios of 17 ± 1 in *ice-9c* (step-heated) and 20 ± 1 in *ice-9d* (crushed). The olivine (separates *ice-9a, -9b, -9c, -9d*) is hosted by glass (*ice-9g-1, -g2*) with $^3He/^4He$ ratios of $17 \pm 1(R_a)$ (step-heat) to $19 \pm 1(R_a)$ (crush) that are similar to the values in *ice-9c* and *-9d*. Compared with the results from this study, Burnard et al. [19] obtained significantly lower $^3He/^4He$ ratios ($13.7R_a$) from crushed olivine, but the ratios from crushed glass ($16.8 \pm 0.2(R_a)$) are similar to those from this study. A contribution from a cosmogenic component of ^3He in *ice-9a* and *-9b* to explain the relatively high $^3He/^4He$ ratios is considered unlikely because sample *ice-9* was obtained from a cliff face in an active quarry and is likely to have been well shielded. These results, together with those reported by Burnard et al. [19], emphasise the variability of the helium isotopic compositions at this locality.

3.2. Neon

The ^{22}Ne abundance in olivine ranges from 1×10^{-12} to 2×10^{-11} cm^3 STP/g and that in glass ranges from 2×10^{-11} to 3×10^{-10} cm^3 STP/g (Table 2). Overall, there is a rough negative correlation between neon isotopic ratios and neon concentration in the samples; the samples with relatively high neon concentrations tend to show neon isotopic ratios close to the atmospheric values. A similar correlation can be recognised in the neon isotope data from Icelandic basalt glasses previously measured by Harrison et al. [24]. These correlations may simply reflect increasing amounts of atmospheric noble gases obscuring the relatively small amounts of mantle noble gases in the magma.

The neon isotope data from this study are plotted on a neon three-isotope diagram in Fig. 3.
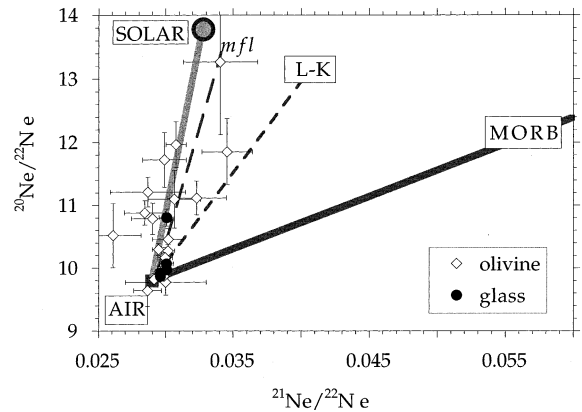
Fig. 3. Neon three-isotope plot, with step-heating and crushing results from a total of 11 samples, or 12 olivine and 10 glass separates. No total gas ratios are shown. The air–solar mixing trend, the mass fractionation line from air (mfl), the Loihi–Kilauea (L–K) trend [2] and the MORB trend [36] are shown for reference. Uncertainty is 1σ.

The neon isotopic ratios from the samples analysed lie on or near one of two trends (Fig. 3). Six samples, not including replicates, have gas fractions released by step-heating or crushing with isotopic compositions that lie on an air–solar mixing trend within one σ uncertainty ($n = 13$ gas fractions) or within two σ uncertainties ($n = 3$ gas fractions). These data are also distinct from the neon isotopic composition in the atmosphere ($^{21}Ne/^{22}Ne = 0.029$; $^{20}Ne/^{22}Ne = 9.8$) by more than two σ uncertainties. These samples (Fig. 3) include both olivine and glass separates from the replicates of sample *ice-9*. Also included are the results from analyses of olivine separates *ice-3a, -3b, -19a, -19b, -30, -32.1a* and *-34* (Table 2). The neon isotopic compositions lying on the air–solar mixing line in mantle-derived samples have not been found previously and are the most significant results of this study.

Neon isotopic ratios of gases released by crushing or step-heating from a few Icelandic samples lie near the MORB trend. Although many of the neon isotopic ratios are quite close to the atmospheric composition, several of these analyses have very small uncertainties and suggest a MORB-like noble gas component may be present. Glass separates from three samples have neon isotopic ratios from individual step-heating or crushing ex-

tractions that lie near the MORB trend in the neon three-isotope plot, with compositions that are distinct from the neon composition in the atmosphere by at least two σ uncertainties (Fig. 3). These are: *ice-18b* (900°C), *ice-18g2* (700°C), *-19a* (900°C) and *-32.2g1* (1500°C). The remaining gas fractions released by step-heating or crushing ($n = 6$) are within two σ of the atmospheric ratios. These near-atmospheric isotopic ratios probably reflect the exchange of atmospheric neon with mantle-derived neon in the magma prior to or during eruption.

As might be expected from the neon isotopic compositions in individual gas fractions described above, the neon isotopic compositions of the total gas released from each sample also show near-solar and MORB-like compositions (Fig. 4). The total gas ratios from five samples (*ice-3* (*-a*, *-b*), *-9* (*-a*, *-b*, *-g1*, *-g2*), *-19* (*-b*), *-30* and *-34*) lie close to the air–solar mixing trend within one σ uncertainty, on a slope that is steeper than the Hawaiian correlation line [2] and have $^{20}Ne/^{22}Ne$ ratios that are greater than the atmospheric ratio of 9.8 by more than two σ uncertainties. This indicates

that the Icelandic plume has a higher proportion of solar to nucleogenic neon than the Hawaiian plume. Total gas ratios from glass separates from four samples (*ice-18* (*-b* and *-g2*), *-47*, *-54* and *-55*) lie near the MORB trend. These samples are close to the atmospheric ratio, but have very small uncertainties such that the $^{21}Ne/^{22}Ne$ ratios are distinct from the atmospheric ratio by more than one σ uncertainty (Fig. 4, inset). The neon isotopic ratios near the air–solar mixing trend and the MORB trend from different samples in this study may indicate that Icelandic basalts contain mixtures of various mantle components. The explanation for preservation of the neon isotopic ratios that lie on or near the air–solar mixing line will be the main focus of Section 4.

4. Discussion

The observed neon isotopic ratios from Icelandic basalts lying on or near the air–solar mixing line imply that a primordial solar neon component trapped within the Earth has remained relatively unchanged over the past 4.5 Ga. Preservation of solar isotopic neon ratios in the silicate mantle is unexpected because the production of time integrated $^{21}Ne^*$ in the mantle, from the Wetherill reactions [34] might be expected to increase the $^{21}Ne/^{22}Ne$ ratio to a value well above the primordial solar ratio [3]. The measured neon isotopic ratio will be indistinguishable from the solar neon isotopic ratio if the concentration of solar neon is relatively high compared with that of time integrated $^{21}Ne^*$, owing to either a high solar neon concentration or a very low U+Th concentration in the neon source region. Near-solar neon isotopic ratios may result from: (1) the preservation of a primitive mantle component with a Ne_{solar} concentration that is sufficiently high such that it overwhelms the amount of $^{21}Ne^*$ produced by the decay of U and Th (i.e. a mantle source with a high $[Ne_{solar}]/[U+Th]$ ratio) or (2) the extraction of solar noble gases from the Earth's outer core, which is assumed to have a very low U and Th content such that the production of $^{21}Ne^*$ over the age of the Earth is negligible.
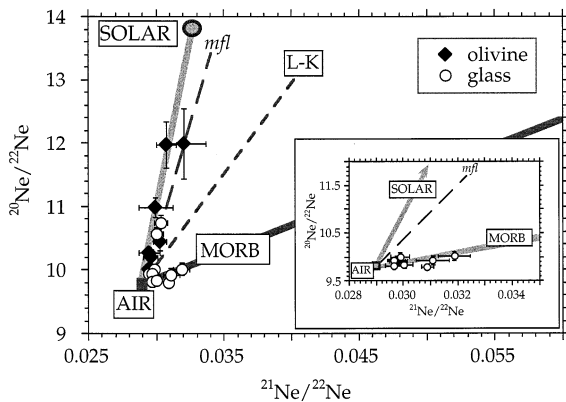
Fig. 4. Neon three-isotope plot showing the composition of the combined gases released from step-heating or crushing extractions (the total gas ratio). One σ uncertainty is shown. Inset: expanded neon three-isotope plot, showing the total ratios from four glass samples and two olivine samples that have neon isotopic compositions on or near the MORB trend. Four samples have neon isotopic ratios that are distinct from the atmospheric composition by $> 1\sigma$ uncertainty (*ice-18* (*-b* and *-g2*), *-47*, *-54* and *-55*). One σ uncertainty is shown.

4.1. Ratio of solar to nucleogenic neon in the MORB and Iceland mantle sources

To evaluate whether the solar neon isotopic ratios are preserved in a part of the Icelandic plume source mantle that has a high $[Ne_{solar}]/[U+Th]$ ratio, it is convenient to compare the composition of the Icelandic plume source with that of the MORB source, which is known to have been largely degassed and is therefore expected to have a comparatively low $[Ne_{solar}]/[U+Th]$ ratio. The relative degree of degassing of solar gases from the Icelandic plume source and MORB source mantle can be obtained by calculating the ratio of solar to nucleogenic neon in basalts from the two sources. The neon isotopic ratio of the mantle is a mixture of the preserved initial solar neon $(^{21}Ne/^{22}Ne)_{solar}$ and the nucleogenic neon $(^{21}Ne*/^{22}Ne*)$ produced in the mantle over the Earth's history; it can be calculated using:

$$(^{21}Ne/^{22}Ne)_{mantle} =$$

$$(^{21}Ne_{solar} + {}^{21}Ne*)/(^{22}Ne_{solar} + {}^{22}Ne*) \qquad (1)$$

The amount of $^{21}Ne*$ that needs to be added to the solar $^{21}Ne/^{22}Ne$ ratio to produce the observed $^{21}Ne/^{22}Ne$ ratio in the MORB source can be calculated, using a simplified version of Eq. 1. The addition of $^{22}Ne*$ has little effect on the observed ratio because the $(^{21}Ne/^{22}Ne)_{solar}$ ratio (0.0328) is orders of magnitude lower than the nucleogenic $^{21}Ne*/^{22}Ne*$ production ratio of 48 [35] so that changes in the $^{21}Ne/^{22}Ne$ ratio are almost entirely caused by addition of $^{21}Ne*$. Consequently, $^{22}Ne*$ may be neglected so that the right hand side of the equation is approximated by $(^{21}Ne_{solar} + {}^{21}Ne*)/(^{22}Ne_{solar})$. Eq. 1 may then be solved for $^{21}Ne*/^{22}Ne_{solar}$ as follows [2]:

$$^{21}Ne*/^{22}Ne_{solar} =$$

$$(^{21}Ne/^{22}Ne)_{mantle} - (^{21}Ne/^{22}Ne)_{solar} \qquad (2)$$

Using a MORB $^{21}Ne/^{22}Ne$ end-member ratio of 0.0744 [36] (the extrapolated value of the $^{21}Ne/^{22}Ne$ ratio at a solar $^{20}Ne/^{22}Ne$ ratio of 13.8 ± 0.1 [26]) and a solar $^{21}Ne/^{22}Ne$ ratio of 0.0328 ± 0.0005 [26], Eq. 2 yields $^{21}Ne*/^{22}Ne_{solar} \approx 0.042$.

The ratio of solar to nucleogenic neon in the Icelandic plume source is expected to be higher than in the MORB source, because the measured Iceland neon isotopic ratios of some samples lie within experimental error of the air–solar mixing line. To obtain the mantle $^{21}Ne/^{22}Ne$ ratio from the measured ratios, the component of atmospheric neon must first be subtracted from the measured value by extrapolating the $(^{21}Ne/^{22}Ne)_{measured}$ ratio to the $(^{20}Ne/^{22}Ne)_{solar}$ ratio of 13.8. For example, the measured neon ratios for sample *ice-9g2* lie near the air–solar mixing line, with a $^{21}Ne/^{22}Ne$ ratio of 0.0304 ± 0.0005 (1.7% uncertainty) and a $^{20}Ne/^{22}Ne$ ratio of 10.74 ± 0.13 (1.2% uncertainty) (Table 1). At a $^{20}Ne/^{22}Ne$ ratio of 13.8, the extrapolated $^{21}Ne/^{22}Ne$ ratio is about 0.035. The uncertainties in the extrapolated $^{21}Ne/^{22}Ne$ ratio are obtained by extrapolating the maximum and minimum $^{21}Ne/^{22}Ne$ ratios (0.0299 and 0.0309, respectively, prior to extrapolation), obtained from the measured uncertainties, along a line from the atmospheric ratio to the solar $^{21}Ne/^{22}Ne$ ratio. Following extrapolation, the maximum $^{21}Ne/^{22}Ne$ ratio is estimated to be 0.0375 and the minimum is 0.0328. Because the Icelandic mantle source region must contain some U and Th, it should contain some nucleogenic neon. The value of 0.0375 constrains the maximum proportion of nucleogenic neon that is likely to be present in the Icelandic plume source region. The results from other Icelandic samples with neon ratios near the air–solar mixing line would yield similar average neon ratios, but owing to their larger uncertainties they place poorer constraints on the maximum and minimum values of the $^{21}Ne/^{22}Ne$ ratio in the plume source.

From Eq. 2, the estimated maximum $^{21}Ne*/^{22}Ne_{solar}$ ratio for the Icelandic plume is 0.0047. This is a measure of the $^{21}Ne*$ required to shift the $^{21}Ne/^{22}Ne$ ratio from the solar to the maximum permitted ratio of 0.0375. The relative concentrations of solar neon in the Icelandic plume source and the MORB source can be obtained from the ratio of $(^{21}Ne*/^{22}Ne_{solar})_{MORB}/(^{21}Ne*/$

$^{22}Ne_{solar})_{Iceland}$ and is equal to 9 (0.042/0.0047). This shows that the proportion of solar neon in the Icelandic plume source is at least nine times greater than in the MORB source, provided that the uranium and thorium contents in the MORB and the Icelandic plume sources are similar.

4.2. Is the Icelandic mantle plume source solar neon-enriched or (U+Th)-depleted?

The higher $^{22}Ne_{solar}/^{21}Ne*$ ratios in the Iceland plume source relative to the MORB source may be caused by a lower U+Th concentration in the Icelandic plume source region, a higher relative solar neon concentration or both. Differences in the U+Th concentrations in the MORB and Icelandic plume sources alone are unlikely to explain the higher $^{22}Ne_{solar}/^{21}Ne*$ ratio in the Iceland plume source for the following reason. Neodymium and strontium isotopic systematics for MORBs (e.g. [37]) and Icelandic basalts [38] show evidence of time-integrated depletion of incompatible elements in both source regions relative to the primitive mantle composition, but the MORB source is more depleted than the Icelandic source. Uranium and thorium, which are typical incompatible elements, are therefore expected to be more depleted in the MORB source than the Icelandic source. If the higher $^{22}Ne_{solar}/^{21}Ne*$ ratios in Icelandic basalts relative to MORBs are due to differences in U+Th, the Icelandic plume source would need to be even more depleted in U+Th than the MORB source. Considering that most Icelandic basalts have experienced less time integrated depletion in incompatible elements than MORB, this possibility appears unlikely.

4.3. Preservation of primitive undegassed mantle

The MORB source has a $^{40}Ar/^{36}Ar$ ratio of at least 40 000 [39–41], markedly higher than the atmospheric value of 295. This difference requires at least the upper part of the Earth's mantle to have undergone a massive degassing event early in its history, before a significant amount of ^{40}K (half-life = 1.25×10^9 years) had decayed to ^{40}Ar [42]. The upper mantle is estimated to have lost

much of its ^{36}Ar in the first 1 Ga of Earth history [43] and is likely also to have lost a similarly large amount of its primordial solar neon during this time. Following the early massive degassing event, ^{40}Ar continued to be produced in the mantle by the decay of ^{40}K (e.g. [43]). A major question that remains is whether this early degassing event also caused extensive degassing of the lower mantle (cf. [44–47]).

Given that at least the upper mantle has undergone a massive early degassing event, followed by continuous degassing, a key question is whether some primitive undegassed mantle could be preserved in the mantle for 4.5 Ga. Continuous degassing occurs via partial melting of the mantle and creates a strongly degassed mantle component that is later recycled and stirred back into the mantle by convection. The result is a hybrid mantle comprised of two end-member components: a strongly degassed recycled component [48] and a much less degassed original primitive mantle component [47,49]. Because partial melting of the mantle is confined to the low pressure zone at the top of the mantle, only a small fraction of the previously undegassed mantle can degas at a given time. Furthermore, the material entering the zone of melting will be a random mixture of primitive undegassed mantle and degassed mantle. Consequently, although the fraction of primitive undegassed mantle will decrease with time, the modern mantle can be expected to contain a small but finite amount of primitive undegassed material ([50] and references therein). The scale of these undegassed mantle domains will decrease with time as they are continually thinned by stirring in the mantle.

The concept that primitive, unmelted domains may exist in the modern mantle is controversial. Primitive mantle is expected to be characterised by chondritic abundances of refractory lithophile trace elements, ε_{Nd} and ε_{Sr} values of zero, and Pb isotopes that lie on the geochron (e.g. [37]). If material with this composition exists in the modern mantle, no evidence for it has been found in the thousands of OIB and MORB samples that have been analysed for radiogenic isotopes. The strontium, neodymium and lead isotopic data therefore appear to preclude the possibility that

zones of primitive undegassed mantle exist on a scale equal to or greater than the zone of melting sampled by basalts. Radiogenic isotope results, however, do not preclude the possibility that regions of primitive undegassed mantle exist within the Icelandic plume source region, provided that the scale of these primitive mantle domains is small compared with the total volume of mantle processed to produce the erupted basalts. If the concentrations of Nd, Sr and Pb in the primitive mantle component are of the same order as in the degassed mantle component, the isotopic compositions of the erupted basalts will lie on mixing arrays between the various isotopic mantle end-members that are sampled by the plume. Radiogenic isotope results will not necessarily provide a definitive test for the presence or absence of a primitive, undegassed mantle component under these circumstances.

The concentration of solar neon contained in relatively primitive undegassed mantle that remains in the lower mantle is likely to be greater than the concentration of solar neon in the upper mantle source of MORBs. One reason is that partial melting occurs in the low pressure region of the upper mantle, so that the degassed mantle residue from partial melting is more likely to be stirred into the adjacent upper mantle than it is into the more distant lower mantle. A second factor is that the viscosity of the mantle increases with pressure and is believed to be about a factor of 30 higher in the lower mantle than it is in the upper mantle [51]. Stirring of the degassed mantle with the undegassed mantle therefore is expected to take longer in the lower mantle than in the upper mantle. Because the Iceland plume source region contains at least nine times more solar neon than the MORB source, it is unlikely to originate within the upper mantle. In comparison, the Hawaiian plume source, with a mantle end-member $^{21}Ne/^{22}Ne$ ratio of 0.0400 [2], has a fraction of solar neon that is only about (0.042/0.0072) six times greater than the MORB source (Eq. 2) and about (0.0072/0.0047) half the amount in the Icelandic plume source. Clearly, the concentration of solar neon in mantle plumes is heterogeneous, which is not unexpected if solar neon is stored in viscous, poorly stirred lower mantle.

Seismic studies have found evidence of a column of hot mantle extending from below Iceland well into the lower mantle (e.g. [13] and references therein) and it is possible that the Iceland plume originates from the thermal boundary layer that is believed to overlie the core [14].

In summary, the neon data suggest that the Earth's mantle still contains a small amount of relatively primitive undegassed material, which likely exists in the lower mantle source of the Icelandic plume. This source region has a high solar neon abundance compared with the upper mantle MORB source. An alternative, but less likely, possibility is that the Icelandic plume obtained its helium and, by inference, solar neon, from the core as discussed by Macpherson et al. [52]. However, as there are no experimental data for helium and neon to support the mechanisms proposed by Macpherson et al. [52] for incorporating helium and neon into the core, any suggestion that neon has been stored in the core remains highly speculative.

5. Conclusions

The neon isotopic ratios measured on some Icelandic samples are the most primitive reported so far from terrestrial mantle-derived samples. These neon data suggest that a small amount of primitive, undegassed material is present in the lower mantle source of the Icelandic plume, which contains much more solar neon than the upper mantle MORB source. The amount of solar neon in mantle plumes appears to be variable because the Hawaiian plume has a proportion of solar neon that is less than that in the Icelandic plume (assuming that the U and Th contents in these reservoirs are similar).

The near-solar neon isotopic ratios are expected to be coupled with near-solar helium isotopic ratios, but this is not observed. Instead, the solar-like neon isotopic ratios are associated with lower $^{3}He/^{4}He$ ratios of 15 to $\sim 30R_a$, interpreted to indicate decoupling of helium and neon during the generation and eruption of the magmas.

The solar-like neon isotopic ratios in some Icelandic basalts have important implications for

mantle convection models because they suggest that the mantle is highly heterogeneous in terms of noble gas concentrations. The Icelandic plume is unlikely to originate from the upper mantle, which is well-mixed and has a less solar-like $^{21}Ne/^{22}Ne$ ratio than the solar end-member in the Icelandic plume. The neon and helium characteristics of the Iceland plume are most consistent with a plume source deep in the lower mantle, a conclusion consistent with recent seismic studies of Iceland [15]. The alternative possibility, that noble gases are stored in the outer core, is considered highly speculative.

Acknowledgements

Appendix A. Methods

Sample preparation

Olivine separates from seven samples were obtained by crushing whole rock samples with a jaw crusher, followed by sieving into fractions of 420 μm–1 mm and 1–2.36 mm, magnetic separation, density separation using heavy liquids and hand picking to remove altered or compound grains. The 420 μm–1 mm size fraction was used for the noble gas analyses, as indicated in Table 1. Prior to analysis most samples were treated ultrasonically in 7% HF for 10 min to remove any

alteration products, followed by optional treatment in 13% HCl for 5 min. These treatments were followed by three or more ultrasonic rinses of at least 15–30 min each in distilled water, acetone, methanol and ethanol. Samples were then dried in an oven for approximately 8 h at 60°C.

Glass samples were from quenched rims of subglacially erupted pillow basalts. Glass separates from six samples were prepared by crushing rock fragments with a mortar and pestle, followed by sieving into fractions of 1–2.36 mm (used for crushing experiments) and 420 μm–1 mm (used for step-heating experiments). Glass separates were then cleaned in the same manner as olivines, but without the acid treatment (because the acids etch the glass surfaces), then handpicked to remove altered, oxidised or compound fragments.

Noble gas analytical methods

Apart from the details of the methods described below, the analytical methods for noble gas analyses are similar to those described in [2,53].

Step-heating experiments

Samples are step-heated because previous studies have shown that atmospheric gases are mainly released in the low temperature steps and mantle components in the high temperature steps. Prior to sample analysis, the following procedure was used. After baking the noble gas extraction system and prior to running blanks, the furnace (tantalum tube and molybdenum liner) was outgassed at 1850°C for up to 1 h. Blanks run at 1800°C were applied to both 1800 and 900°C sample runs. Using the 1800°C blank for the 900°C step did not result in a significant difference in the isotopic ratios of the samples following blank corrections. The range in 1800°C blanks prior to olivine runs are as follows: $^4He = 5 \times 10^{-12}$ to 2×10^{-10} cm³ STP; $^{20}Ne = 2 \times 10^{-12}$ to 3×10^{-11} cm³ STP. Because the gas concentrations in glasses are substantially higher than in olivine, less time was spent outgassing the furnace prior to glass runs than prior to olivine runs. Blanks prior to step-

heating glasses were run at 1600°C. The average blanks were 3×10^{-11} to 5×10^{-11} cm^3 STP for ^{4}He and 5×10^{-12} to 2.6×10^{-11} cm^3 STP for ^{20}Ne. A 10% uncertainty was assumed in the value of the blanks.

Crushing experiments

Crushing experiments are useful to assess the difference between gases trapped in inclusions or vesicles versus those in the matrix of glasses or minerals, particularly where a cosmogenic component may be present in the matrix. The crusher was run for 5 min at 300 strokes/min for both samples and blanks. The range in blanks for crushing experiments were: ^{4}He $= 4 \times 10^{-11}$ to 8×10^{-10} cm^3 STP; ^{20}Ne $= 4 \times 10^{-12}$ to 3×10^{-11} cm^3 STP. Following crushing, the sample chamber of the crusher was heated to 100°C in order to drive off re-adsorbed gases from the freshly exposed sample surface. After the gas extraction, the sample was recovered and sieved; the crushed sample yield was taken as the fraction less than < 150 μm, which was typically about 50% of the total sample mass loaded.

Detection limits

The helium and neon abundances measured in the gas released from the samples are well above the detection limits calculated from the sensitivity and collector noise of the mass spectrometer [2]. The helium data were filtered by plotting the ^{3}He/^{4}He ratio versus the absolute abundance of ^{3}He or ^{4}He. Samples with helium amounts below 3×10^{-9} cm^3 STP ^{4}He and 7×10^{-14} cm^3 STP ^{3}He were discarded because there was a change in the measured ^{3}He/^{4}He ratios from relatively constant values above these gas amounts, but a marked increase at lower amounts. This relates to an increase in the uncertainties of the measurements at low gas amounts. The neon data were filtered to discard samples with measured amounts of ^{22}Ne (e.g. before blank subtraction) below 1.5×10^{-12} cm^3 STP and ^{21}Ne amounts below 8×10^{-14} cm^3 STP, because the isotopic ratios

were unreasonably scattered below these gas amounts.

Neon isotope analysis

Possible pressure effects on the neon mass discrimination factors were examined by measuring neon isotopic ratios in air neon stored in a gas pipette (one aliquot contains 2.7×10^{-9} cm^3 STP of ^{20}Ne) by expansion to reduce the amounts analysed by two orders of magnitude. The neon mass discrimination factors were constant (within $\sim 1\%$) over this pressure range. Thus, no corrections for pressure effects needed to be applied to neon isotope ratios measured on gases released from the samples in this study. Mass discrimination factors used to reduce the data are obtained from the average of neon isotopic ratios from 8 to 16 separate analyses of the heavy gas standard.

The resolution of the Daly collector on the VG5400 mass spectrometer is 600, hence corrections are needed for interferences from peaks that require resolution greater than 600 for separation; in particular, corrections need to be made for ^{40}Ar^{2+} and H$_2^{18}$O$^+$ on ^{20}Ne; CH$_2$CO^{2+} on ^{21}Ne, and CO$_2^{2+}$ on ^{22}Ne. For the interference corrections, blank subtractions and reference isotope changes, we used algorithms that keep track of correlated errors in isotopic ratios [2]. To demonstrate how errors associated with such corrections are propagated, neon data obtained from *ice-9g2* are used in the following example. The measured and unprocessed ^{21}Ne/^{20}Ne and ^{22}Ne/^{20}Ne ratios (reference isotope: ^{20}Ne) were 0.002787 ± 0.000027 ($\pm 0.9\%$) and 0.092165 ± 0.000068 ($\pm 0.07\%$), respectively (^{20}Ne/^{22}Ne $= 10.85$; ^{21}Ne/^{22}Ne $= 0.0302$). The quoted errors are one standard deviation, which include uncertainties in the regression calculation of time-zero extrapolation to gas inlet time. The fractions from (1) CO$_2^{2+}$, (2) CH$_2$CO^{2+}, (3) ^{40}Ar^{2+} and (4) H$_2^{18}$O$^+$ subtracted from the measured amounts of the neon isotopes in *ice-9g2* were: (1) $4.5 \times 10^{-3} \pm 0.5 \times 10^{-3}$; (2) $1.8 \times 10^{-4} \pm 0.4 \times 10^{-4}$; (3) $1.4 \times 10^{-3} \pm 0.3 \times 10^{-3}$ and (4) $1.1 \times 10^{-4} \pm 0.4 \times 10^{-4}$, respectively. After the corrections for interferences and mass discrimination (uncertainties de-

termined by repeated analysis of the air neon from the gas pipette), the $^{21}Ne/^{20}Ne$ and $^{22}Ne/^{20}Ne$ ratios were 0.002826 ± 0.000032 (1.1%) and 0.0937 ± 0.0011 (1.2%) (for reference isotope $^{20}Ne = 1.96 \pm 0.09 \times 10^{-9}$ cm^3 STP/g, $^{20}Ne/^{22}Ne = 10.67$ and $^{21}Ne/^{22}Ne = 0.0302$). The amount of ^{20}Ne in the blank was 7.86×10^{-12} cm^3 STP ($\pm 10\%$) and atmospheric isotopic ratios were used for blank subtraction. After the blank correction the $^{22}Ne/^{20}Ne$ ratio was equal to 0.0931 ± 0.0011 and $^{21}Ne/^{20}Ne = 0.002829 \pm 0.000031$; for reference isotope $^{20}Ne = 1.94 \pm 0.09 \times 10^{-9}$ cm^3 STP/g, the $^{20}Ne/^{22}Ne$ and $^{21}Ne/^{22}Ne$ ratios are 10.74 ± 0.07 and 0.0304 ± 0.0005, as listed in Table 2.

In addition to the standard corrections for mass interferences, the ^{20}Ne peak was scanned for possible interferences from $H^{19}F$ associated with cleaning the samples in HF. Although the $^{40}Ar^{2+}$ peak could be seen as a small flat peak overlapping part of the ^{20}Ne peak, there was no evidence for interference from HF. Mass 19 was also scanned for possible evidence of F, but no peak was visible.

References

[1] H. Craig, J.E. Lupton, Primordial neon, helium, and hydrogen in oceanic basalts, Earth Planet. Sci. Lett. 31 (1976) 369–385.

[2] M. Honda, I. McDougall, D.B. Patterson, A. Doulgeris, D.A. Clague, Noble gases in submarine pillow basalt glasses from Loihi and Kilauea, Hawaii: a solar component in the Earth, Geochim. Cosmochim. Acta 57 (1993) 859–874.

[3] M. Honda, I. McDougall, D.B. Patterson, Solar noble gases in the Earth: the systematics of helium–neon isotopes in mantle derived samples, Lithos 30 (1993) 257–265.

[4] M.D. Kurz, W.J. Jenkins, S.R. Hart, D. Clague, Helium isotopic variations in volcanic rocks from Loihi Seamount and the Island of Hawaii, Earth Planet. Sci. Lett. 66 (1983) 388–406.

[5] D.R. Hilton, K. Gronvold, C.G. Macpherson, P.R. Castillo, Extreme $^3He/^4He$ ratios in northwest Iceland: constraining the common component in mantle plumes, Earth Planet. Sci. Lett. 173 (1999) 53–60.

[6] D.R. Hilton, K. Hammerschmidt, G. Loock, H. Friedrichsen, Helium and argon isotope systematics of the central Lau Basin and Valu Fa Ridge: evidence of crust/mantle interactions in a back-arc basin, Geochim. Cosmochim. Acta 57 (1993) 2819–2841.

[7] K.A. Farley, E. Neroda, Noble gases in the Earth's mantle, Annu. Rev. Earth Planet. Sci. 26 (1998) 189–218.

[8] J.E. Lupton, Terrestrial inert gases: isotope tracer studies and clues to primordial components in the mantle, Ann. Rev. Earth Planet. Sci. 11 (1983) 371–414.

[9] J.R. Smallwood, R.S. White, T.A. Minshull, Sea-floor spreading in the presence of the Iceland plume the structure of the Reykjanes Ridge at 61°40′N, J. Geol. Soc. London 152 (1995) 1023–1029.

[10] R.S. White, J.W. Bown, J.R. Smallwood, The temperature of the Iceland plume and origin of outward-propagating V-shaped ridges, J. Geol. Soc. London 152 (1995) 1039–1045.

[11] J.G. Schilling, M. Zajac, R. Evans, T. Johnston, W. White, J.D. Devine, R. Kingsley, Petrologic and geochemical variations along the Mid-Atlantic Ridge from 29°N to 73°N, Am. J. Sci. 283 (1983) 510–586.

[12] R. Poreda, J.-G. Schilling, H. Craig, Helium and hydrogen isotopes in ocean-ridge basalts north and south of Iceland, Earth Planet. Sci. Lett. 78 (1986) 1–17.

[13] H. Bijwaard, Tomographic evidence for a narrow whole mantle plume below Iceland, Earth Planet. Sci. Lett. 166 (1999) 121–126.

[14] R.W. Griffiths, I.H. Campbell, Stirring and structure in mantle starting plumes, Earth Planet. Sci. Lett. 99 (1990) 66–78.

[15] D.V. Helmberger, L. Wen, X. Ding, Seismic evidence that the source of the Iceland hotspot lies at the core–mantle boundary, Nature 396 (1998) 251–255.

[16] S.P. Jakobsson, J. Jonsson, F. Shido, Petrology of the Western Reykjanes Peninsula, Iceland, J. Petrol. 19 (4) (1978) 669–705.

[17] I. McDougall, N.D. Watkins, G.P.L. Walker, L. Kristjansson, Potassium–argon and paleomagnetic analysis of Icelandic lava flows: limits on the age of anomaly 5, J. Geophys. Res. 81 (1976) 1505–1512.

[18] I. McDougall, L. Kristjansson, K. Saemundsson, Magnetostratigraphy and geochronology of northwest Iceland, J. Geophys. Res. 89 (1984) 7029–7060.

[19] P.G. Burnard, F.M. Stuart, G. Turner, N. Oskarsson, Air contamination of basaltic magma: implications for high $^3He/^4He$ mantle Ar isotopic composition, J. Geophys. Res. 99 (1994) 17709–17715.

[20] M. Condomines, K. Gronvold, P.J. Hooker, K. Muehlenbachs, R.K. O'Nions, N. Oskarsson, E.R. Oxburgh, Helium, oxygen, strontium and neodymium isotopic relationships in Icelandic volcanics, Earth Planet. Sci. Lett. 66 (1983) 125–136.

[21] M. Kurz, P.S. Meyer, H. Sigurdsson, Helium isotopic systematics within the neovolcanic zones of Iceland, Earth Planet. Sci. Lett. 74 (1985) 291–305.

[22] D.R. Hilton, K. Gronvold, R.K. O'Nions, E.R. Oxburgh, Regional distribution of ^3He anomalies in the Icelandic crust, Chem. Geol. 88 (1990) 53–67.

[23] D.R. Hilton, K. Gronvold, A.E. Sveinbjornsdottir, K.

Hammerschmidt, Helium isotope evidence for off-axis degassing of the Icelandic hotspot, Chem. Geol. 149 (1998) 173–187.

[24] D. Harrison, P. Burnard, G. Turner, Noble gas behaviour and composition in the mantle: constraints from the Iceland plume, Earth Planet. Sci. Lett. 171 (1999) 199–207.

[25] M. Honda, I. McDougall, D.B. Patterson, A. Doulgeris, D.A. Clague, Possible solar noble gas component in Hawaiian basalts, Nature 349 (1991) 149–151.

[26] J.-P. Benkert, H. Baur, P. Signer, R. Wieler, He, Ne, and Ar from the solar wind and solar energetic particles in lunar ilmenites and pyroxenes, J. Geophys. Res. 98 (1993) 13147–13162.

[27] R.G. Tronnes, Basaltic melt evolution of the Hengill volcanic system, SW Iceland, and evidence for clinopyroxene assimilation in primitive tholeiitic magmas, J. Geophys. Res. 95 (1990) 15893–15910.

[28] H. Risku-Norja, Gabbro nodules from a picritic pillow basalt, Midfell, SW Iceland, Nordic Volcanol. Inst. Prof. Paper 8501, 1985.

[29] D. Lal, Production of ^{3}He in terrestrial rocks, Chem. Geol. 66 (1987) 89–98.

[30] D. Lal, Cosmic ray labeling of erosion surfaces: in situ nuclide production rates and erosion models, Earth Planet. Sci. Lett. 104 (1991) 424–439.

[31] D. Lal, In situ-produced cosmogenic isotopes in terrestrial rocks, Annu. Rev. Earth Planet. Sci. 16 (1988) 355–388.

[32] I.A. Sigurdsson, Primitive Magmas in Convergent Margins and at Oceanic Spreading Ridges: Evidence from early formed Phenocryst Phases and their Melt Inclusions, Ph.D. thesis, University of Tasmania, 1994.

[33] T.H. Hansteen, Multi-stage evolution of the picritic Maelifell rocks, SW Iceland: constraints from mineralogy and inclusions of glass and fluid in olivine, Contrib. Miner. Petrol. 109 (1991) 225–239.

[34] G.W. Wetherill, Variations in the isotopic abundances of neon and argon extracted from radioactive minerals, Phys. Rev. 96 (1954) 679–683.

[35] I. Yatsevich, M. Honda, Production of nucleogenic neon in the Earth from natural radioactive decay, J. Geophys. Res. 102 (1997) 10281–10288.

[36] P. Sarda, T. Staudacher, C.J. Allègre, Neon isotopes in submarine basalts, Earth Planet. Sci. Lett. 91 (1988) 73–88.

[37] A.W. Hofmann, Mantle geochemistry: the message from ocean volcanism, Nature 385 (1997) 219–229.

[38] C. Hemond, N.T. Arndt, U. Lichtenstein, A. Hofmann, The heterogeneous Iceland plume: Nd–Sr–O isotopes and trace element constraints, J. Geophys. Res. 98 (1993) 16833–16850.

[39] C.J. Allègre, T. Staudacher, P. Sarda, Rare gas systematics: formation of the atmosphere, evolution and structure of the Earth's mantle, Earth Planet. Sci. Lett. 81 (1986–1987) 127–150.

[40] P. Burnard, D. Graham, G. Turner, Vesicle-specific noble gas analyses of 'popping rock': implications for primordial noble gases in Earth, Science 276 (1997) 568–571.

[41] M. Moreira, J. Kunz, C. Allegre, Rare gas systematics in popping rock: isotopic and elemental compositions in the upper mantle, Science 279 (1998) 1178–1181.

[42] R. Hart, L. Hogan, J. Dymond, The closed-system approximation for evolution of argon and helium in the mantle, crust and atmosphere, Chem. Geol. (Isotope Geosci.) 52 (1985) 45–73.

[43] G. Turner, The outgassing history of the Earth's atmosphere, J. Geol. Soc. London 146 (1989) 147–154.

[44] R.K. O'Nions, I.N. Tolstikhin, Behaviour and residence times of lithophile and rare gas tracers in the upper mantle, Earth Planet. Sci. Lett. 124 (1994) 131–138.

[45] D. Porcelli, G.J. Wasserburg, A unified model for terrestrial rare gases, in: K.A. Farley (Ed.), Volatiles in the Earth and Solar System, American Institute of Physics, New York, 1995, pp. 56–69.

[46] G.F. Davies, Geophysically constrained mantle mass flows and the ^{40}Ar budget: a degassed lower mantle?, Earth Planet. Sci. Lett. 166 (1999) 149–162.

[47] J. PhippsMorgan, Thermal and rare gas evolution of the mantle, Chem. Geol. 145 (1998) 431–445.

[48] C.J. Allègre, D.L. Turcotte, Implications of a two-component marble cake mantle, Nature 323 (1986) 123–127.

[49] T.W. Becker, J.B. Kellogg, R.J. O'Connell, Thermal constraints on the survival of primitive blobs in the lower mantle, Earth Planet. Sci. Lett. 171 (1999) 351–365.

[50] G.F. Davies, Geophysical and isotopic constraints on mantle convection: an interim synthesis, J. Geophys. Res. 89 (1984) 6017–6040.

[51] M. Gurnis, G.F. Davies, The effect of depth-dependent viscosity on convective mixing in the mantle and the possible survival of primitive mantle, Geophys. Res. Lett. 13 (1986) 541–544.

[52] C.G. Macpherson, D.R. Hilton, J.M. Sinton, R.J. Poreda, H. Craig, High ^{3}He/^{4}He ratios in the Manus backarc basin: Implications for mantle mixing and the origin of plumes in the western Pacific Ocean, Geology 26 (1998) 1007–1010.

[53] T. Matsumoto, M. Honda, I. McDougall, S. O'Reilly, Noble gases in anhydrous lherzolites from the Newer Volcanics, southeastern Australia: a MORB-like reservoir in the subcontinental mantle, Geochim. Cosmochim. Acta 62 (1998) 2521–2533.